

# Microfabricated Atomic Frequency References

S. Knappe, P. Schwindt, V. Shah, L. Hollberg, J. Kitching  
Time and Frequency Division  
NIST  
Boulder, CO, USA  
knappe@boulder.nist.gov

L. Liew, J. Moreland  
Electromagnetics Division  
NIST  
Boulder, CO, USA

**Abstract**—We report on the fabrication of a physics package for a chip-scale atomic clock with a volume of  $9.5 \text{ mm}^3$ , consuming 75 mW of power. The design is described in detail and is strongly motivated by the goal of wafer-level fabrication and assembly. A fractional frequency instability of  $2.4 \times 10^{-10}$  at one second of integration is demonstrated; the long-term drift is  $-2 \times 10^{-8}/\text{day}$ . We discuss the performance of the clock at short and long integration times as well as its power consumption, and suggest possible improvements.

**Keywords**- Atomic frequency reference, chip-scale atomic clock, vapor cell, wafer-level integration, frequency instability

## I. INTRODUCTION

This paper discusses recent progress in the development of a microfabricated physics package for a highly miniaturized atomic frequency reference [1]. The goal of this project is to develop a chip-scale atomic clock with a volume below  $1 \text{ cm}^3$ , a fractional frequency instability below  $10^{-11}$  at one hour of integration time, and power consumption of less than 30 mW. This could enable the integration of atomic timekeeping into portable, battery-operated devices, where better long-term stability is needed than is currently available with compact quartz crystal oscillators. Such applications could include jam-resistant GPS receivers [2], secure wireless communication systems [3], and synchronization of telecommunication networks [4].

The development of the physics package is a critical step for these chip-scale clocks. Our design implements the precision laser spectroscopy that probes the atoms in a volume of about  $10 \text{ mm}^3$ . A microwave local oscillator is then locked onto the resonance signal derived from the atom spectroscopy. Recent advances in the development of thin-film resonators [5,6,7], as well as SiC nano-resonators [8] have enabled small devices operating in the gigahertz range. These devices might be suitable for the development of local oscillators for integration into chip-scale atomic clocks. Furthermore, the control electronics to stabilize the laser and cell temperatures, as well as the laser and local oscillator frequencies, are not complex. They could be implemented as low-power devices with a small footprint in the form of an application-specific integrated circuit (ASIC) or digital microprocessor.

## II. FABRICATION

The physics package developed at NIST, shown in Fig. 1, consists entirely of parts that can be fabricated by use of standard processes in microelectromechanical systems (MEMS); this fabrication method also allows for wafer-level integration. At the base of the physics package a VCSEL is mounted, emitting light vertically at a wavelength of 852 nm, matching the cesium resonance line. With its high modulation bandwidth and low threshold current, it constitutes a reliable light source requiring only 4 mW of DC power and 70  $\mu\text{W}$  of microwave power at 4.6 GHz to transfer 60 % of the emitted light power into the two first-order modulation sidebands. This light is attenuated to 12  $\mu\text{W}$  by two neutral-density (ND) filters integrated into a micro-optics assembly. A microlens made by ink-jet deposition of optical epoxy collimates the light into a beam of diameter  $\sim 250 \mu\text{m}$ . At the top of the micro-optics assembly the light is circularly polarized by a quartz plate of thickness 70  $\mu\text{m}$ . After exiting the micro-optics assembly, the beam passes through a vapor cell containing the cesium atoms [9,10]. At the top of the stack, a photodiode chip is mounted to detect the light transmitted through the cell.

The vapor cell was made by first etching square holes of side 0.9 mm through a silicon wafer, 1 mm thick, using an isotropic KOH etch. A piece of borosilicate glass 200  $\mu\text{m}$  thick was then attached to one side of the silicon wafer by anodic bonding at 500 V and 300  $^\circ\text{C}$  [11]. After a mixture of  $\text{BaN}_6$  and  $\text{CsCl}$  is deposited into this preform, it is transferred to a high-vacuum system. A second piece of borosilicate glass is then placed against the open side, and the preform is heated to 170  $^\circ\text{C}$  to decompose the chemical mixture into  $\text{BaCl}$ ,  $\text{Cs}$ , and  $\text{N}_2$ . The  $\text{N}_2$  is pumped off and the vacuum chamber is backfilled with a mixture of 14 kPa of nitrogen and 11 kPa of argon. The top glass piece is then anodically bonded to the silicon at 300 V and 300  $^\circ\text{C}$ . Finally, the cell is removed from the chamber and diced to a square of 1.45 mm side.

In order to increase the Cs vapor pressure inside the cell, the cell was heated to 80  $^\circ\text{C}$ . For this, two glass substrates of thickness 125  $\mu\text{m}$ , and coated with a thin film of indium tin oxide (ITO), are placed directly onto the two cell windows. When a current is sent through the two ITO heaters, relatively

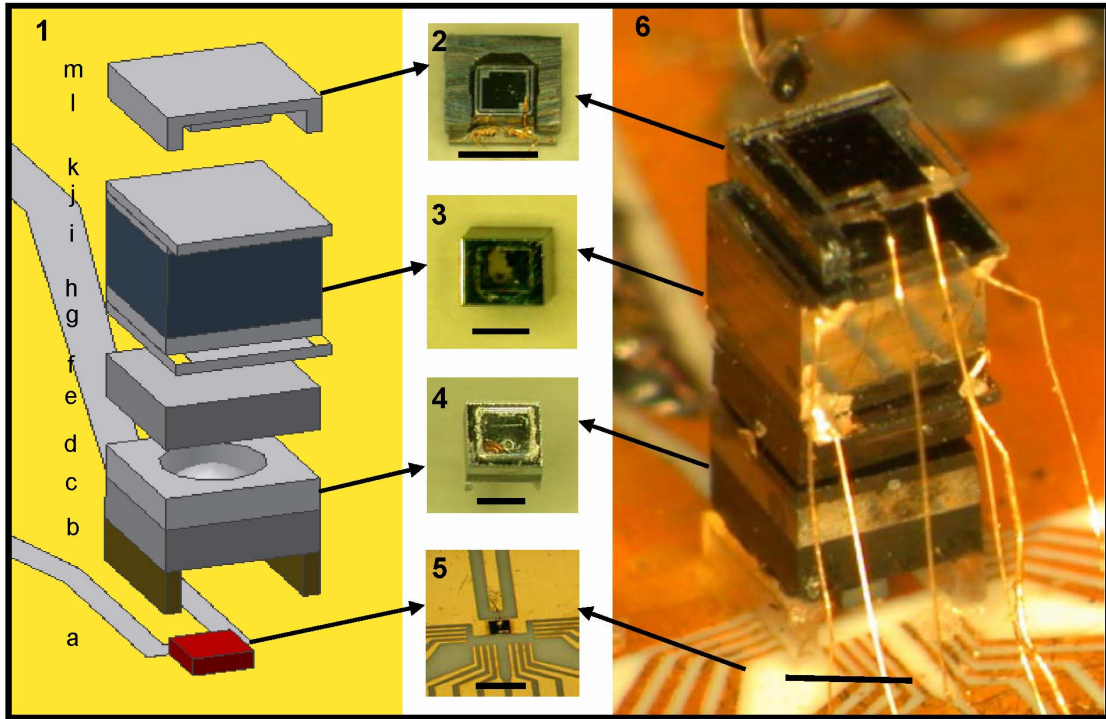


Figure 1. The physics package of the microfabricated atomic frequency reference. Left: Schematic assembly with (a) VCSEL, (b) glass (500  $\mu\text{m}$ ), (c) ND filter (500  $\mu\text{m}$ ), (d) spacer/lens (375  $\mu\text{m}$ ), (e) quartz (70  $\mu\text{m}$ , not shown), (f) ND filter (500  $\mu\text{m}$ ), (g) glass/ITO (125  $\mu\text{m}/30\text{ nm}$ ), (h) glass (200  $\mu\text{m}$ ), (i) Si (1000  $\mu\text{m}$ ), (j) glass (200  $\mu\text{m}$ ), (k) glass/ITO (125  $\mu\text{m}/30\text{ nm}$ ), (l) Si (375  $\mu\text{m}$ ), (m) glass (125 $\mu\text{m}$ ). Total height: 4.2 mm, width and depth: 1.5 mm. Center: Photographs of the: (2) photodiode assembly, (3) cell assembly, (4) optics assembly, and (5) laser assembly Right: the full atomic-clock physics package realized as a microchip. The black lines in the photographs indicate 1 mm.

uniform heating of the cell is achieved, keeping the windows slightly hotter than the rest of the cell to prevent the Cs from coating the windows. This first system required 69 mW of power to heat the cell; most of the heat is lost by conduction through the lower spacer unit and the six gold wire bonds in roughly equal parts. The remaining power is lost by convection and radiation through the air. Finite-element modeling of the setup indicates that the power to heat the cell could be reduced to below 15 mW by using better insulation between the cell and the baseplate and by vacuum capping the device with an evacuated enclosure [12].

### III. COHERENT POPULATION TRAPPING

The clock draws on coherent population trapping (CPT) [13] to excite a microwave resonance in cesium atoms. It allows for a simple spectroscopic setup to measure the ground-state hyperfine splitting of the atoms at 9.2 GHz without the use of a microwave cavity. Two light fields resonant with the transitions from the two ground-state hyperfine components to the same excited  $P_{3/2}$  state can pump the atoms into a so-called dark state, if the difference frequency between the two light fields is exactly equal to the hyperfine splitting frequency of the ground state. (Fig. 2) Under this condition the atoms do not absorb light and therefore the optical power of the light transmitted through the cell increases.

The bichromatic light field is produced by direct modulation of the injection current of a vertical-cavity surface-emitting laser (VCSEL) at 4.6 GHz, a frequency equal to one-half the ground-state hyperfine splitting of Cs. The two first-order sidebands are then tuned into resonance with the atomic  $D_2$ -line at 852 nm. When scanning the modulation frequency and consequently the difference frequency of the two light fields, a narrow bright line will appear in the spectrum of the transmitted light (Fig. 3). The modulation frequency can then be locked onto this resonance, and thus provide a stable output frequency of the clock.

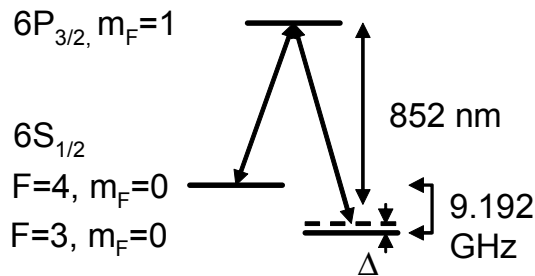


Figure 2. Optical excitation of Cs microwave transition using coherent population trapping. The two optical fields at 852 nm are resonant with the two transitions from the two ground-state hyperfine components with the same excited  $P_{3/2}$  state. A ground-state coherence out of phase with the driving light fields can be induced in this way such that the atoms become transparent to the optical fields. The resonance can be seen by monitoring the DC transmitted light power while scanning the difference frequency between the light fields.

#### IV. PERFORMANCE

The CPT resonance is detected by monitoring the transmitted light power as the modulation frequency is scanned about the first subharmonic (4.6 GHz) of the difference frequency between the two  $m_F = 0$  ground states (9.2 GHz) (Fig. 3). The resonance amplitude, normalized to the Doppler absorption background is only 0.91 %. The primary reason for the low contrast lies in the excited-state hyperfine structure of the  $D_2$  line, where single-photon transitions reduce the lifetime of the dark state [14]. Using the  $D_1$  line of  $^{85}\text{Rb}$  contrasts of more than 15 % have been measured [15]. A secondary reason is that the atoms are roughly equally distributed among the Zeeman levels of the ground state; thus only  $1/8^{\text{th}}$  of the atoms contribute to the 0-0 dark state. Initial experiments designed to demonstrate high stability indicate that normalized amplitudes on the order of 5 % can be obtained when operating on the  $^{87}\text{Rb}$   $D_1$  line even in microfabricated cells with volumes of  $1 \text{ mm}^3$ . The measured width of the Cs CPT resonance is 7.1 kHz and is dominated by power broadening. Secondary contributions to the width, accounting for 2.9 kHz, are the result of Cs atoms diffusing to the cell wall as well as Cs-Cs, Cs- $\text{N}_2$ , and Cs-Ar spin-exchange collisions [16].

An error signal can be generated from this CPT resonance, which signal can be used to lock the synthesizer producing the initial 4.6 GHz signal onto the atomic resonance. The output frequency stabilized in this manner is then compared to the signal from a more stable reference. A time series of such a frequency measurement is shown in the inset of Fig. 4. From this, a short-term fractional frequency instability of  $2.4 \times 10^{-10}/\sqrt{\tau}$  can be deduced (Fig. 4). At short times it is limited in roughly equal parts by shot-noise on the photodetector current, excess amplitude noise on the laser light, and laser frequency noise, which is converted into amplitude noise by the atomic absorption profile. Improving the contrast or width of the CPT

resonance, by use of the  $D_1$  line, for example, would directly translate into an improved short-term stability.

The long-term stability of the clock is limited by a frequency drift of  $-2 \times 10^{-8}/\text{day}$ , which is easily visible in the inset of Fig. 4. Most likely this drift is a result of the cell filling process using  $\text{BaN}_6$ . Over time, the nitrogen used as a buffer gas slowly recombines with the barium residue left over from the chemical reaction on the interior cell walls. This reaction reduces the buffer gas pressure, and since nitrogen produces a shift of the hyperfine splitting frequency of roughly  $62 \text{ Hz/kPa}$  [17], the clock output frequency drops as the nitrogen is slowly depleted. In order to avoid this drift, a buffer gas mixture of inert gases could be used, since they do not react with barium. Another possibility is to directly deposit cesium into the cells without chemical residues. First experiments using both of these techniques indicate that the long-term drift can be drastically reduced. When the linear drift is removed in post-processing the data, the Allan deviation reaches a minimum of  $2.5 \times 10^{-11}$  at 250 s. The remaining long-term stability is consistent with residual changes of the cell temperature. The hyperfine frequency shift due to collisions between Cs and buffer gas atoms is temperature dependent since the velocity of the atoms changes. The sign of this temperature shift depends on the buffer gas used. By carefully choosing the right mixture of buffer gases which shift the frequency in opposite directions the temperature dependence can be cancelled in first order [15, 18]. Nevertheless, in order to reach a frequency stability of  $10^{-11}$  at 1 h, the temperature stability of the cell will need to be improved.

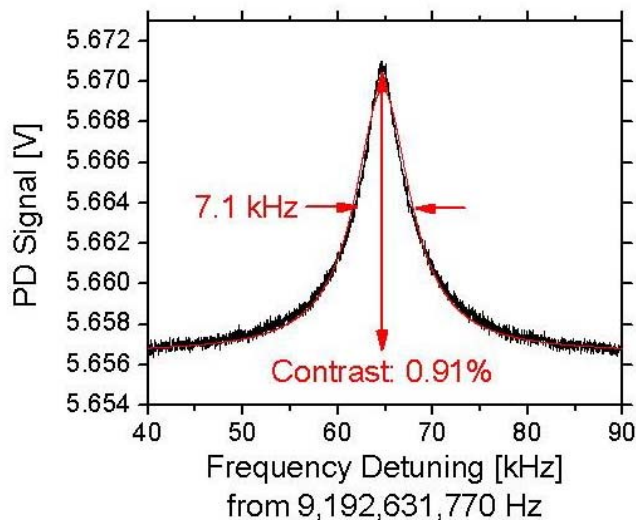


Figure 3. CPT resonance. The light transmitted through the vapor cell is plotted as a function of difference frequency between the two resonant light fields.

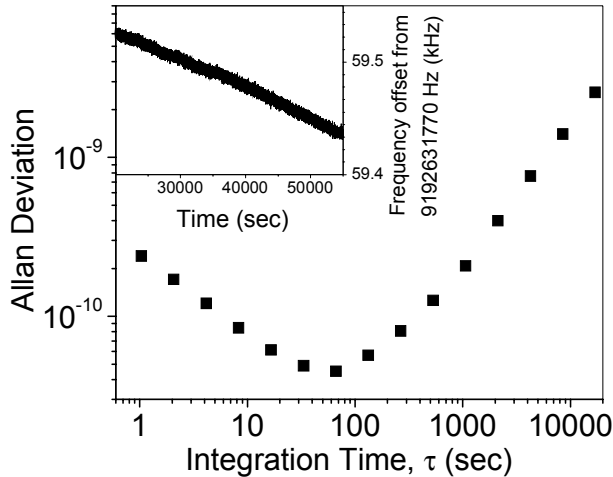


Figure 4. Fractional frequency instability of the microfabricated frequency reference as a function of integration time, as estimated by the Allan deviation. Inset: Output frequency of the frequency reference as a function of time.

One advantage of the physics package design shown, in Fig. 1, is the possibility of wafer-level assembly. Each layer of the device could be fabricated as an array of many identical components on a wafer (Fig. 5). These wafers could then be stacked together and subsequently diced into individual physics packages. This would allow the production of a large number of identical devices with the same process sequence, largely reducing production cost. This could open the possibility of making chip-scale atomic clocks an inexpensive commercial product.

#### CONCLUSION

We have demonstrated a chip-scale atomic clock physics package in a volume of  $9.5 \text{ mm}^3$ . The measured fractional frequency instability of  $2.4 \times 10^{-10}/\sqrt{\tau}$  is consistent with a frequency instability of  $10^{-11}$  at 1 h, if improvement in the long-term drift can be realized. The current device consumes 75 mW of power, not including the baseplate power, and calculations indicated that it can be reduced to below 20 mW, making these clocks good candidates for use in battery-operated devices. The entire physics package is designed to be integrated at the wafer level. All individual components could be fabricated as large arrays on wafers, reducing the fabrication costs of each single clock.

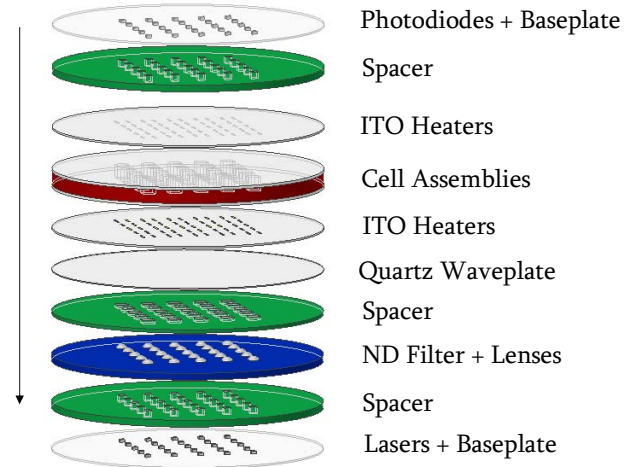


Figure 5. Wafer-level assembly. On each of the wafers, an array of individual clock components is fabricated. From bottom to top the wafers host VCSELS on baseplates, spacers, ND filters and lenses, spacers, quarter waveplates, heaters, cell assemblies, heaters, spacers, photodiodes and mounts. The wafers can then be bonded together and subsequently diced into separate clock physics packages.

#### REFERENCES

- [1] S. Knappe, V. Shah, P. Schwindt, L. Hollberg, J. Kitching, L. Liew, and J. Moreland, "Amicrofabricated atomic clock", *Appl. Phys. Lett.*, vol. 85, pp. 1460-1462, 2004
- [2] H. Fruehauf, "Fast "direct-P(Y)" GPS signal acquisition using a special portable clock" Proceedings of the 33rd Annual Precise Time and Time Interval Meeting, Long Beach, CA 27-29 November 2001, 369-370.
- [3] J. Vig, "Military applications of high-accuracy frequency standards and clocks", *IEEE Trans. UFFC*, vol. 40, pp. 522-527, 1993
- [4] J. A. Kusters and C.A. Adams, "Performance requirements of communication base station time standards", *RF Design*, pp. 28-38, 1999
- [5] K.M. Lakin, and J.S. Wang, "Acoustic bulk wave composite resonators", *Appl. Phys. Lett.*, vol 38, pp. 125-127, 1981
- [6] W. Pang, H. Zhang, H. Yu, and E.S. Kim, "Electrically tunable and switchable film bulk acoustic resonator", in these proceedings.
- [7] F. Stratton, D. Chang, D. Kirby, R. Joyce, T.-Y. Hsu, and H. Kubena, "A MEMS-based quartz resonator technology for GHz applications", in these proceedings.
- [8] X. M. H. Huang, C. Zorman, M. Mehregany, and M. L. Roukes, "Nanodevice motion at microwave frequencies", *Nature*, vol. 421, p. 496, 2003
- [9] L. Liew, S. Knappe, J. Moreland, H.G. Robinson, L. Hollberg, and J. Kitching, "Microfabricated alkali atom vapor cells", *Appl. Phys. Lett.*, vol. 48, pp. 2694-2696, 2004
- [10] S. Knappe, V. Velichansky, H.G. Robinson, L. Liew, J. Moreland, J. Kitching, and L. Hollberg, "Atomic vapor cells for miniature frequency references", *Proc. 2003 IEEE Int. FCS and PDA Exhib. Jointly 17<sup>th</sup> EFTF*, pp. 31-32
- [11] P. R. Wallis and D. I. Pomeranz, "Field assisted glass-metal sealing", *J. Appl. Phys.*, vol. 40, pp. 3946-3949, 1969
- [12] J. Kitching, S. Knappe, L.-A. Liew, P. Schwindt, V. Shah, J. Moreland, and L. Hollberg, "Power dissipation in a vertically-integrated chip-scale atomic clock", in these proceedings.
- [13] E. Arimondo, "Coherent Population Trapping in Laser Spectroscopy", *Progress in Optics XXXV*, E. Wolf, ed., pp. 257-354, 1996

- [14] M. Zhu, "Coherent population trapping-based frequency standard and method for generating a frequency standard incorporating a quantum absorber that generates the CPT state with high frequency," U.S. Patent 6,395,916 (March 19, 2002).
- [15] M. Stähler, R. Wynands, S. Knappe, J. Kitching, L. Hollberg, A. Taichenachev, and V. Yudin, "Coherent population trapping resonances in thermal Rb-85 vapor: D-1 versus D-2 line excitation", *Opt. Lett.*, vol. 27, pp. 1472-1474, 2002
- [16] J. Kitching, S. Knappe, and L. Hollberg, "Miniature vapor-cell atomic-frequency references", *Appl. Phys. Lett.*, vol. 81, pp. 553-555, 2002
- [17] J. Vanier and C. Audoin, *The Quantum Physics of Atomic Frequency Standards*. (A. Hilger, Philadelphia, 1989)
- [18] S. Knappe, J. Kitching, L. Hollberg, R. Wynands, "Temperature dependence of coherent population trapping resonances", *Appl. Phys. B*, vol. 74, pp. 217-222, 2002

The authors gratefully acknowledge valuable advice from H. G. Robinson and help with fabrication of the baseplate from Y. Chang and Y.C. Lee. This work was supported by the Microsystems Technology Office of the US Defense Advanced Research Projects Agency (DARPA). This work is a contribution of NIST, an agency of the US Government, and is not subject to copyright.